Anisotropic PP and PSv Prestack Depth Migration of 4C (OBC) Seismic Data, Offshore Trinidad

Tony Johns*
WesternGeco, Houston, TX, United States
Johns5@slb.com

and

Raul Sarmiento
EOG Resources, Houston, TX, United States

In November 2004, EOG Resources acquired an ocean-bottom cable (OBC) 4C swath survey across the Pamberi-1 well location in the Lower Reverse L block of the Columbus basin, eastern offshore Trinidad. The purpose of the 4C survey was to evaluate the potential of long-offset multicomponent technology for resolving lithology and stratigraphic detail in an area perturbed by shallow gas, overpressure and illumination shadows from normal regional faults and major anticlinal ridge trends acting as pressure seals. The motivation from EOG for attempting this was because a conventional 3D towed-streamer survey acquired the previous year failed to adequately image the target reflectors comprising the reservoir under the main growth fault.

Details of the P- and PS_v-wave processing of this dataset through anisotropic prestack time migration were previously described (Johns et al., 2006) in which it was demonstrated there existed a qualitative correlation between derived parameters and attributes from P and S_v anisotropic migration velocities and known regional geology. This observation was quite remarkable considering that only a limited effort to constrain or validate parameters was performed. Under the “Future work” section of the previous publication, it was suggested that further data quality enhancement in preparation for more quantitative rock property classification, calibrated to wells, could only be achieved after prestack depth imaging.

In this paper, we present precisely that next phase in the 4C processing, advancing the P- and PS_v-wave data through anisotropic prestack depth migration, using cell-based tomography with a top-down pseudo layer-stripping approach. The Pamberi-1 well information was used to constrain the anisotropy in the shallow section, with the deeper, spatial trend away from the proximity of the well determined from the anisotropy derived previously in the time processing.

Prior to proceeding with the anisotropic depth imaging, the magnitude of shear splitting (or, birefringence) from the presence of azimuthal anisotropy is first examined to assess its potential impact on the radial rotated P-S signal. The shear-wave splitting analysis revealed a principal angle of polarization that was closely aligned with the regional stress direction delineated by the major faults blocks acting as pressure seals.

Azimuthal Anisotropy

Azimuthal anisotropy, as opposed to polar anisotropy (VTI/TTI) accounted for in traveltime ray tracing of prestack depth migration, can cause shear waves to split into fast (S_1) and slow (S_2) components, propagating orthogonal to each other. Depending on the difference between S_1 and S_2 and thus the magnitude of azimuthal anisotropy, the polarization could result in reduced resolution of the radial (source-receiver azimuth) PS rotated signal due to the destructive interference of fast and slow shear energy. Numerous papers on shear splitting have been previously published, such as Probert and Kristiansen (2003), which demonstrate the importance of identifying and measuring azimuthal anisotropy on PS data.

Evidence of shear splitting was initially noted from inspection of the PS radial and transverse QC stacks with simple asymptotic binning. Detrimental dimming on the radial PS stack was not evident; however it was still considered important to quantify the magnitude of potential shear splitting from azimuth rotation analyses on common receiver gathers. These analyses were performed on 500-m limited-offset 3D azimuth bins, every 1 km, along the northernmost receiver line of the swath. Despite this 4C survey being acquired predominantly inline, the inner 500-m offset range is comprised of a full 3D distribution of azimuths and could be utilized to identify and measure the polarization of the converted-wave data from analysis of shear splitting.

Prior to examining the azimuthal variation on the converted-wave data, it is first necessary to verify the vector orientation and fidelity of the OBC detectors, as recorded by the individual geophone accelerometer components, Z, X, and Y. The detector orientation is confirmed by analyzing the relative energy or polarization of the direct arrivals and computing the rotation angle about each of the Z, X, and Y axes. Thereafter, common 45° azimuth traces from each of the horizontal X and Y component receiver gathers are generated and are found to exhibit impressive correlation, consistent with the OBC system's reputation for excellent vector fidelity. The visual comparison was so convincing that further hodogram analysis was deemed unnecessary.

Once satisfied with vector fidelity so that integrity of the shear splitting analysis is assured, attention then focused on deriving full 360° azimuthal analyses on the offset-limited common receiver gathers using sets of raw X-Y component and radial-transverse rotated data. Polarization analysis was conducted on the transverse data through detection of polarity flips every 90° change in azimuth using a "snowflakes" time-slice display scheme as described by Bale et al. (2000), and elegantly exploited by Olofsson et al. (2003) and Probert and Kristiansen (2003). In the absence of azimuthal anisotropy, a rotation is not observed and the maximum "snowflake" response aligns with the common acquisition coordinate system. The polarization results at different time slices on the southern set of three receiver locations, where the radial sinusoidal effect is clearly evident, revealed a noticeable rotation in the principal axis of polarization below 1.0 s. From analysis of the earliest arrivals of the radial over the sinusoidal responses at each receiver analysis location it is possible to distinguish between S_1 and S_2. Results indicated the fast orientation of polarization is parallel to the regional normal fault trend and is consistent with the known dominant stress fields within each major fault block.

Analysis over the central and northern set of receiver gathers show less residual coherent energy on the transverse and minimal azimuthal variation in velocity. These results are consistent with the transverse stack and indicate less evidence of shear splitting. The polarization analyses at different time slices below 1.0 s reveal a rotation of only a few degrees. Therefore, the strongest evidence of shear splitting, as hinted on the transverse stacks, is constrained to the southern one-third of the swath on the upthrown side of the major fault and is less prevalent elsewhere in the survey.

Anisotropic Prestack Depth Migration

Knowledge of the restrained impact of the azimuthal anisotropy on the PS data provided the necessary confidence to use the preprocessed radial (source–receiver direction) rotated data as input to the PS PrSDM. Special compensation from Alford rotation with layer-stripping correction was not considered essential. For the P-wave, the selected input was the preprocessed PZ data that had been summed using a non-linear PZ combination technique (Moldoveanu, 1996) to deghost receiver-side water-layer multiples.

In the application of PrSDM, a Kirchhoff depth imaging algorithm was selected, that had been routinely adapted to account for PS_v-waves with anisotropy and dual surfaces (for the different source and receiver datums from OBC acquisition). Compensation for anisotropy was based on Thomsen's weak anisotropy relationship for a VTI medium (Thomsen, 1986), using parameters δ and ε. Anisotropy has a greater influence on the description of the velocity for S-wave than with P-wave because the ratio of the square of the vertical V_p/V_s ratio is >> 1 in the expression for the S_v velocity as a function of phase angle, vertical P- and S-wave velocity and Thomsen's anisotropy parameters. Of course, the challenge was deriving a valid velocity model to apply in the Kirchhoff PrSDM. That is, a model that produces flat common image point (CIP) gathers across positive and negative offsets, for optimized stack response, and correlates equivalent events on both P- and PS_v-wave depth sections at the correct depth confirmed by well data. For this project, the velocity analysis of residual moveout on CIP gathers was performed using a cell-based (gridded) 3D reflection tomography approach. Gridded models allow more flexibility to represent velocity variations that are not easily interpreted from structural dependency in the seismic and are applicable to regions such as the Gulf of Mexico and offshore Trinidad. Due to the inability to perform P- and S-wave tomographic updates simultaneously, the initial priority was to focus on the PZ data and derive a good V(P) model before proceeding to run tomography on the PS data. The work flow that was adopted is summarized as follows:

1. Prestack depth migrate the PZ data with an initial smoothed isotropic P-wave velocity field, derived from the previous time processing.
2. Update isotropic V(P) iteratively from residual velocities using CIP tomography to the flatten gathers.
3. Update V(P) with anisotropy to tie depths at the Pamberi-1 well location deriving both δ and ε to flatten gathers over the shallow depth range of the well.
4. Incorporate the Annie η (Sayers and Johns, 1999) VTI model from the previous time processing to represent the anisotropy below and beyond the proximity of the well. In this instance it was decided to hold δ constant with ε spatially varying.
5. Migrate PZ with the updated anisotropic V(P) model.
6. Migrate PS data anisotropically with the updated anisotropic V(P) and initial smoothed V(S) derived from the anisotropic PS_v time processing.
7. Update V(S) model iteratively from residual velocities using CIP tomography to flatten PS gathers.
8. Revise V(S) to register PZ and PS events in depth. Modify ε and δ as per the original VTI η field.
9. Reiterate with decreasing scalar wavelength using the PS tomography to solve for residual anisotropy (ε and δ) until solution converges.

The methodology was carried out adopting a top-down layered approach, prioritizing the shallow section first before progressing deeper. For each iteration in the P- and PS_v-wave workflow, the positive and negative offsets were migrated separately to allow determining the residual moveout

independently, but solved simultaneously for an update of V(P) in the case of PZ, or V(S) in the case of the PS data. The advantage of having previously performed detailed prestack time processing meant that the V(P) and V(S) starting models were reliable and that an initial spatially varying anisotropic field could be incorporated early into the workflow. The Pamberi-1 well log contained no shear information, so the well tie was performed on P-wave (PZ) data only. Nevertheless, the log provided a derived 1D set of Thomsen parameters over the 3-km depth interval of the well that could be merged with the 3D VTI model from the time processing. Deeper than 3 km it was initially assumed δ=0 with ε equating simply to the spatially varying η parameter, in accordance with the (Thomsen, 1986) equation:

$$\eta = (\varepsilon - \delta) / (1 + 2\delta) \quad (1)$$

The anisotropic Thomsen parameters were further updated after the PZ and PS depth images were registered to determine the depth discrepancy between the two volumes, as per step 8 in the workflow. For this process to be successful, it is crucial to interpret equivalent horizons on both wave modes. This challenge is compounded by the fact that the shear and acoustic reflectivities are generally different, so the key is to identify common geological features, such as faults, and map these to a series of horizons. The event correlations were originally interpreted on the depth-to-time converted sections to validate the implied interval γ_0 ratios. The identified registered horizons were then transferred to the PZ and PS PrSDM sections to deduce the depth discrepancy. A 7% mistie, on average, was measured between the PS and PZ in the 600m to 3400m depth range, requiring pull-up on the PS depth section, equivalent to a reduction in V(S).

Results

Preliminary prestack analysis of the raw and radial rotated converted-wave data indicated evidence of mild shear splitting from azimuthal anisotropy attributable, in part, to dominant regional stress fields delineated by major fault blocks. The advantage of the detectors exhibiting near-perfect cross-component vector fidelity and orientation facilitated the identification and measurement of principal azimuths of shear-wave polarization on the PS data. It was encouraging to observe that the principal azimuth of polarization agreed closely with known regional lateral stress field orientation for the area. The polarization to S_1 and S_2 was restricted to a rotation of 15° or less from the survey's natural acquisition orientation, and appeared to have minimal detrimental impact on the final radially rotated PS data quality.

After several iterations of constrained cell-based tomography with progressively smaller scale lengths (smoothing) and the necessary incorporation of anisotropy, the resultant P- and PS_v-wave PrSDM sections are found to exhibit an enhancement in structural detail and continuity, together with improved P-P to P-S_v correlation of target events, across the main fault (Figure 1). The inclusion of anisotropic (VTI) properties from the previous prestack time processing, subsequently updated after well control and P-P to P-S event registration, produced a significant improvement in PS_v imaging; more so than the impact noted in the P-wave migration. Furthermore, better flattening of the PS_v depth gathers over the entire positive and negative 10-km offset range was observed, across the main fault, which is important for future AVO/inversion work in the extraction of rock property attributes. Although raypath asymmetry (Thomsen, 1999) and lateral heterogeneity is causing significant variation in the PS_v reflectivity, structurally there is a better depth consistency match between the positive- and negative-offset PrSDM sections than that noted on the time-processed data, increasing confidence in the PS_v depth interpretation.

Conclusion

In this paper, we demonstrate for the Pamberi area of the Columbus basin of eastern offshore Trinidad, that further to the improvement over the conventional 3D towed-streamer time imaging from 4C anisotropic prestack time migration (Johns et al., 2006), an incremental enhancement is also possible with anisotropic PrSDM of the P- and PS_v-wave data. Utilizing cell-based tomography to derive anisotropic velocity models, parameterization was further optimized through well control and detailed event registration.

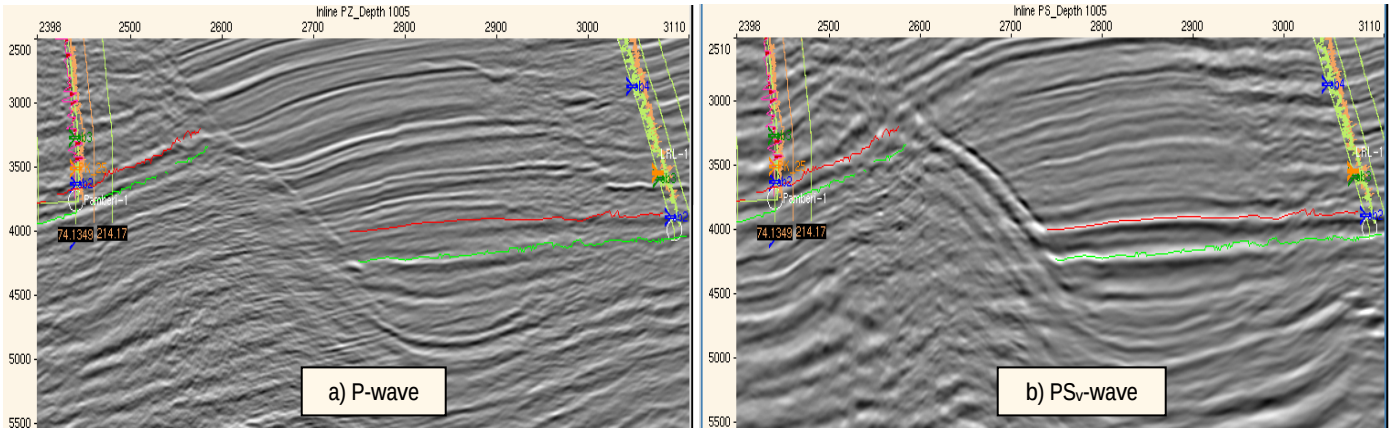

Figure 1. Central inline PrSDM sections from (a) PZ P-wave, and (b) PSv-wave data with correlated depth horizons and well log overlays. The Pamberi-1 well is on the left. The PSv section shows a series of bright events on the downthrown (red and green horizons) which are not clearly visible on the PZ data. An example of where this 4C dataset has identified potential new leads.

References

Johns, T., Vito, C., Clark, R, and Sarmiento, R..: "*Multicomponent OBC (4C) prestack time imaging: Offshore Trinidad, Pamberi, LRL Block",* 76th Annual International Meeting, SEG 2006 expanded abstracts **25**, 1193

Probert, A. and Kristiansen, P.: "*Why is azimuthally anisotropic processing important for multicomponent seismic?*", 73rd Annual International Meeting, SEG 2003 expanded abstracts **22**, 773.

Bale, R., Dumitru, G., and Probert, A.: "*Analysis and stacking of 3D converted wave data in the presence of azimuthal anisotropy",* 70th Annual International Meeting, SEG 2000 expanded abstracts **19**, 1189

Olofsson, B., Probert, A., Kommedal, J., and Olav I. Barkved, O.:"*Azimuthal anisotropy from the Valhall 4C 3D survey",* The Leading Edge **22,** (2003), 1228 - 1235.

Moldoveanu, N.: "*Method for attenuation of reverberations using a pressure-velocity bottom cable*", (1996) US Patent 5,621,700.

Thomsen, L.: "*Weak elastic anisotropy*", *Geophysics* **51,** (1986), 1954-1966.

Sayers, C. and Johns, T.: "*Anisotropic velocity analysis using marine 4C seismic data*", 69th Annual International Meeting, SEG 1999 expanded abstracts **18,** 780.

Thomsen, L., "*Converted-wave reflection seismology over inhomogeneous, anisotropic media*", *Geophysics* **64,** (1999), 678–690.